

Shaping the waveform of entangled photons

Alejandra Valencia,^{*} Alessandro Cerè,[†] Xiaojuan Shi, Gabriel Molina-Terriza,[‡] and Juan P. Torres[§]
ICFO-Institut de Ciències Fotoniques, Mediterranean Technology Park, Castelldefels, 08860 Barcelona, Spain
(Dated: October 26, 2018)

We demonstrate experimentally the tunable control of the joint spectrum, i.e. waveform and degree of frequency correlations, of paired photons generated in spontaneous parametric downconversion. This control is mediated by the spatial shape of the pump beam in a type-I noncollinear configuration. We discuss the applicability of this technique to other sources of frequency entangled photons, such as electromagnetically induced Raman transitions.

PACS numbers:

The quantum description of paired photons includes the spatial shape, the polarization state and the joint spectrum. The later contains all the information about bandwidth, type of frequency correlations and waveform of the two-photon state. Quantum light has been proved to be useful in many quantum information applications and the most appropriate form of the joint spectrum depends on the specific realization under consideration. For example, uncorrelated pairs of photons can be used as a source of heralded single photons with a high degree of quantum purity [1, 2]; the tolerance against the effects of mode mismatch in linear optical circuits can be enhanced by using photons with appropriately tailored waveform shape [3]; the use of frequency-correlated or anticorrelated photons allows erasing the distinguishing information coming from the spectra when considering polarization entanglement [4, 5]; some protocols for quantum enhanced clock synchronization and positioning measurements rely on the use of frequency anticorrelated [6] or correlated photons [7]. Moreover, the entanglement in the frequency domain offers by itself a new physical resource where to explore quantum physics in a high-dimensional Hilbert space [8]. This requires the development of new techniques for the control of the joint spectrum that will allow the generation of multidimensional waveform alphabets.

The most widely used method for the generation of pairs of entangled photons is spontaneous parametric down conversion (SPDC). Notwithstanding, paired photons with the desired joint spectrum may not be harvested directly at the output of the downconverting crystal. The question that arises is how to control independently different aspects of the joint spectrum of entangled paired photons generated in SPDC; importantly, the sought-after techniques should work for any frequency band of interest and any nonlinear crystal.

Various methods have been proposed and developed to control the type of frequency correlations and the bandwidth of downconverted photons. Some of these methods rely on an appropriate selection of the nonlinear crystal length and its dispersive properties [4, 9]. Others are based on SPDC pumped by pulses with angular dispersion [10] or the design of nonlinear crystal superlat-

tices [11]. Noncollinear SPDC has also been propose as a way to tailor the waveform of the downconverted photons [12, 13, 14, 15, 16, 17]. Contrary to the case of collinear SPDC, where the transverse spatial shape of the pump beam translate into specific features of the spatial waveform of the two-photon state; in noncollinear SPDC, the phase matching conditions inside the nonlinear crystal mediates the mapping of spatial features of the pump beam into the joint spectrum of the downconverted photons [18]. This spatial-to-spectral mapping allows to tune independently frequency correlations and the waveform. In this letter, we demonstrate experimentally this mapping and report experiments that demonstrate the feasibility of using noncollinear SPDC as a tool to control the type of frequency correlations using as tunable parameter the size of the pump beam waist and the angle of emission of the downconverted photons. In the past, measurements of the joint spectrum have been reported [5, 19]. However, to the best of our knowledge this is the first time that manipulations of the joint spectrum have been demonstrated experimentally.

Let us consider noncollinear type-I SPDC in a nonlinear crystal of length L cut for non-critical phase matching. The spatiotemporal quantum state of the two-photon pair can be written as $|\psi\rangle = \int d\Omega_s d\vec{q}_s d\Omega_i d\vec{q}_i \Phi(\Omega_s, \Omega_i, \vec{q}_s, \vec{q}_i) |\Omega_s, \Omega_i, \vec{q}_s, \vec{q}_i\rangle$, where $\Phi(\Omega_s, \Omega_i, \vec{q}_s, \vec{q}_i)$ is the mode function or biphoton, which contains all the information about the correlations and waveform properties of the two-photon light. $\Omega_j = \omega_j - \omega_j^0$ are frequency deviations from the central frequencies (ω_j^0), and $\vec{q}_j = (q_{jx}, q_{jy})$ are the transverse wavevectors for the signal (s) and idler (i) photons.

In order to elucidate the frequency correlations and waveform of the SPDC pairs, we consider the joint spectrum, $S(\Omega_s, \Omega_i) = \left| \int d\vec{q}_s d\vec{q}_i \Phi(\Omega_s, \Omega_i, \vec{q}_s, \vec{q}_i) U^*(\vec{q}_s) U^*(\vec{q}_i) \right|^2$, where the function $U(\vec{q}_j)$ describes the spatial mode in which the downconverted photons are projected. For instance, gaussian modes when the downconverted photons are collected with an imaging system followed by single mode optical fibers [20, 21]. Projection into large area modes is equivalent to projection into $\vec{q}_s = \vec{q}_i \simeq 0$, i.e.,

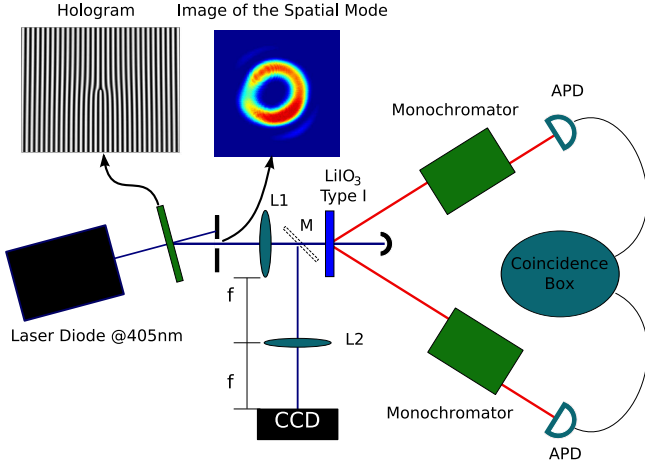


FIG. 1: Sketch of the experimental setup. The LG mode is produced by a computer generated hologram. Photos of the hologram and the diffracted beam are shown. The size of the beam impinging into the crystal is controlled via L1. The downconverted beams are collected into single mode optical fibers and sent through a pair of computer controlled monochromators and APD detectors. Single and coincidence counts are recorded with standard electronics. M is a flipping mirror used to switch from the frequency correlation measurement to the transverse momentum distribution measurement.

$$U(\vec{q}) \propto \delta(\vec{q}).$$

The signal and idler photons travel inside the crystal at an angle $\varphi_s = -\varphi_i = \varphi$ with respect to the direction of propagation of the pump beam. The mode function can then be written as [22]

$$\begin{aligned} \Phi(\Omega_s, \Omega_i, \vec{q}_s, \vec{q}_i) &= E_q(q_{xs} + q_{xi}, \Delta_0) E_\omega(\Omega_s + \Omega_i) \\ &\times \text{sinc}\left(\frac{\Delta_k L}{2}\right) \exp\left\{-i\frac{\Delta_k L}{2}\right\}, \end{aligned} \quad (1)$$

where E_q and E_ω are the spatial shape of the pump beam in the transverse wavevector domain and the pump pulse frequency spectrum, respectively. $\Delta_0 = (q_{sy} + q_{iy}) \cos \varphi - (k_s + k_i) \sin \varphi$ accounts for the phase mismatching along the transverse direction, and $\Delta_k = k_p - (k_s + k_i) \cos \varphi - (q_{sy} + q_{iy}) \sin \varphi$ for the phase matching conditions along the longitudinal direction. k_j is the wavevector for signal, idler, and pump waves. Eq. (1) reveals that for the chosen configuration the spatial properties of the pump, E_q , are mapped into the spectral domain of the downconverted photons, $S(\Omega_s, \Omega_i)$, through the dependence of Δ_0 on the frequency.

To obtain further physical insight, we do a first order Taylor expansion of $k_j(\omega_j^0 + \Omega_j)$ around the central frequencies, and assume large area collection modes ($\vec{q}_s = \vec{q}_i \simeq 0$). The joint spectrum reduces to

$$\begin{aligned} S(\Omega_s, \Omega_i) &= |E_q(0, N_s \sin \varphi \Omega_-)|^2 |E_\omega(\Omega_+)|^2 \\ &\times \exp\left\{-\frac{[\alpha(N_p - N_s) \cos \varphi L]^2}{4} \Omega_+^2\right\}, \end{aligned} \quad (2)$$

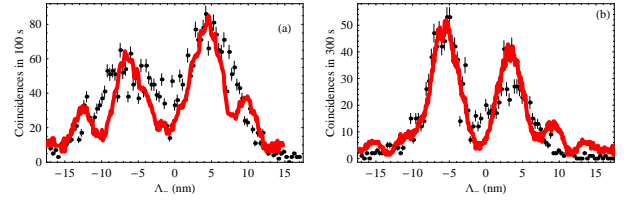


FIG. 2: Comparison of the measured spatial shape of the pump beam in the transverse wavevector domain (solid line), and the measured joint spectral intensity as a function of Λ_- (dots). (a) The pump beam shape is modified with a hologram and, (b) The spatial shape is modified with a thin microscope slab.

where $N_j \equiv dk_j/d\omega_j$ is the corresponding inverse group velocity, $\Omega_+ \equiv \Omega_s + \Omega_i$ and $\Omega_- \equiv \Omega_s - \Omega_i$. We have approximated the phase matching function, $\text{sinc}(\Delta_k L/2)$, by an exponential function that has the same width at the $1/e^2$ of the intensity: $\text{sinc}(bx) \simeq \exp[-(\alpha b)^2 x^2]$, with $\alpha = 0.455$. Notice that the spatial to spectral mapping occurs between the shape of the pump beam along the transverse direction and the frequency shape in the Ω_- axis.

The experimental setup used to demonstrate this mapping is sketched in Fig. 1. A $L = 1$ mm long LiIO₃ crystal, cut for type-I noncollinear degenerate SPDC, is pumped with a high power laser diode (Nichia NDHV220APAE1) centered at $\lambda_p^0 = 405$ nm, with a measured bandwidth of $\Delta\lambda_p \simeq 0.4$ nm. The spatial mode of the laser beam is reduced to Gaussian by a set of cylindrical lenses and a spatial filter. The degenerate down converted photons centered at $\lambda_s^0 = \lambda_i^0 = 810$ nm are produced at an internal angle $\varphi = 17.1^\circ$ (which corresponds to noncritical phase matching) and are imaged into two single mode fibers via two lenses ($f = 11$ mm) placed at 54 cm from the output face of the nonlinear crystal. The output of each fiber is sent through two monochromators (Jobin Yvon MicroHR), and finally sent into single photon counting modules (Perkin-Elmer SPCM-AQR-14-FC). Singles and coincidence counts for the two detectors are recorded and the joint spectrum is measured by scanning both monochromators.

In order to recognize the spatial-to-spectral mapping, we choose pump spatial modes whose transverse momentum distribution poses a clearly identifiable dip in the center. The spatial profile of the pump beam is modified using two different schemes. First, we use a hologram that generates, into its first diffraction order, a vortex beam with topological charge $m = 2$. A picture of the hologram, and the corresponding shape of the pump beam after the hologram, are shown in the inset of Fig. 1. Alternatively, the pump beam is sent to a thin microscope slab that introduced a phase shift over half of the beam. The transverse momentum distribution of the pump, $E_q(0, N_s \sin \varphi \Omega_-)$, can be measured by means of the $2f$ system and a CCD camera. The image from the

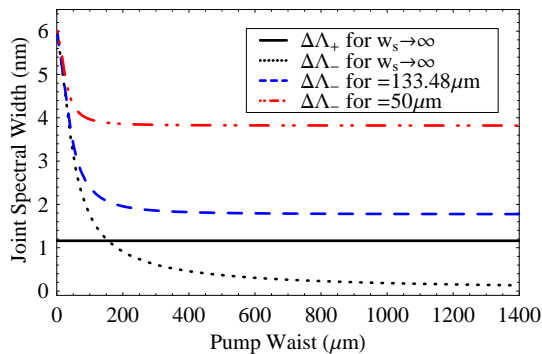


FIG. 3: Spectral widths $\Delta\Lambda_-$ and $\Delta\Lambda_+$ as a function of the pump beam width (W_0). $\Delta\Lambda_-$ is shown for three different values of the spatial collection mode, $W_s = 133.48 \mu\text{m}$, $W_s = 50 \mu\text{m}$ and $W_s \rightarrow \infty$. Since $\Delta\Lambda_+$ does not change significantly with W_s , only $\Delta\Lambda_+$ for $W_s \rightarrow \infty$ is depicted. The intersection between $\Delta\Lambda_-$ and $\Delta\Lambda_+$ for $W_s \rightarrow \infty$ would allow complete tunable control of the type of frequency correlations.

camera relates to the frequency correlations according to $\Lambda_- = 4\pi y / (f N_s \sin \varphi \omega_s^0)$, where y is the spatial coordinate in the transverse direction and $\Lambda_- \equiv \lambda_s^0 \Omega_- / \omega_s^0$.

Figure 2 compares the measured spatial shape of the pump beam in the transverse wavevector domain (solid line), $|E_q(0, N_s \sin \varphi \Omega_-)|^2$, and the measured joint spectrum shape as a function of Λ_- (dots). Fig. 2a shows the results for the case where the pump beam shape is modified with the hologram, and Fig. 2b when the thin microscope slab is used. The matching of the solid lines and the points reveals that the spatial characteristics of the pump beam, $E_q(0, N_s \sin \varphi \Omega_-)$, are mapped into the joint spectrum of signal and idler photons, $S(\Omega_s, \Omega_i)$. As a special feature, we can clearly see that the dip of the spatial pump profile translates into a dip in the joint spectrum at $\Lambda_- = 0$, i.e. $\lambda_s = \lambda_i = 810 \text{ nm}$. Importantly, this technique makes possible to tailor the frequency waveform of the two-photon state independently of the nature of the frequency correlations of the photon pairs.

The possibility of transferring the spatial characteristics of the pump beam into the joint spectrum of the downconverted photons, in principle allows the control of the type of frequency correlations between signal and idler. Let us consider the case in which the pump beam is characterized by a transverse momentum profile $E(\vec{q}_p) \propto \exp[-|\vec{q}_p|^2 W_0^2 / 4]$ and a spectral distribution $E(\Omega_p) \propto \exp[-\Omega_p^2 / (4B_p^2)]$. W_0 and B_p are the beam waist and the bandwidth of the pump beam. Furthermore, signal and idler are projected into the spatial mode $U(\vec{q}_j) \propto \exp[-|\vec{q}_j|^2 W_s^2 / 4]$. The joint spectrum then reads

$$S(\Omega_s, \Omega_i) = \mathcal{N} \exp\left\{-\frac{\Omega_+^2}{2B_+^2}\right\} \exp\left\{-\frac{\Omega_-^2}{2B_-^2}\right\} \quad (3)$$

where

$$B_- = \left[\frac{1}{2B_f^2} + \frac{(N_s \sin \varphi W_0)^2}{1 + 2(W_0 \cos \varphi / W_s)^2} \right]^{-1/2}, \quad (4)$$

$$B_+ = \left[\frac{1}{B_p^2} + \frac{1}{2B_f^2} + \frac{(\alpha L)^2 (N_p - N_s \cos \varphi)^2}{1 + 2(\alpha \sin \varphi L / W_s)^2} \right]^{-1/2} \quad (5)$$

and \mathcal{N} is a normalizing factor. We have also assumed the presence of frequency filters of the form $H(\Omega_{s,i}) \propto \exp\left[-\Omega_j^2 / (4B_f^2)\right]$ in front of the detectors.

The ratio between the distribution widths B_+ and B_- characterizes the type of frequency correlation of the two-photon state: anticorrelated photons are obtained for a pump beam width so that $B_- \gg B_+$, while we get correlated photons when $B_- \ll B_+$. If $B_- = B_+$, we have uncorrelated frequency photons. From Eq. (4), the width B_- mainly depends on the pump beam width and the noncollinear angle. In order to compare with the experimental data, we will work with the variables Λ_- and $\Lambda_+ \equiv \lambda_s^0 \Omega_+ / \omega_s^0$ and to which we associate the width (standard deviation) $\Delta\Lambda_-$ and $\Delta\Lambda_+$, respectively. Fig. 3 shows the dependence of $\Delta\Lambda_-$ on the pump beam waist, W_0 , for different values of W_s . When for a value of W_s , the $\Delta\Lambda_+$ and $\Delta\Lambda_-$ curves cross we have the possibility of generating paired photons anticorrelated ($\Delta\Lambda_+ < \Delta\Lambda_-$), correlated ($\Delta\Lambda_+ > \Delta\Lambda_-$), and even uncorrelated ($\Delta\Lambda_+ = \Delta\Lambda_-$) in frequency by choosing an appropriate values of the pump beam waist.

For the sake of clarity and due to the weak dependence of $\Delta\Lambda_+$ on W_s for a given pump bandwidth, we only plot $\Delta\Lambda_+$ for the ideal case, $W_s \rightarrow \infty$. When comparing the curves for different values of W_s , it is clear that the generation of anticorrelated photons is not greatly affected by the collection modes. Highly frequency anticorrelated photons are obtained for a focused pump and the relationship W_s / W_0 is large so that, effectively, one always projects into a large area mode and, therefore, approaches the condition $\vec{q}_s = \vec{q}_i \simeq 0$. On the other hand, the size of W_s sets a minimum value of the bandwidth of the pump for the generation of uncorrelated or highly correlated frequency two-photon states.

We demonstrate experimentally the feasibility of frequency correlation control exploiting the setup of Fig. 1. In this case, we use a pump with a Gaussian profile and a telescope to modify the pump beam waist. W_0 is measured by means of a beam shaper (Coherent BM-7). For our collection scheme, the imaging relation gives us a collection mode waist, $W_s^{exp} = 133.48 \mu\text{m}$. The upper part of Fig. 4 shows the joint spectra for two different values of W_0 . These are obtained by scanning the two monochromators and recording coincidence counts. A two dimensional Gaussian fit is employed to obtain the bandwidths along Λ_+ and Λ_- of the distribution. Part

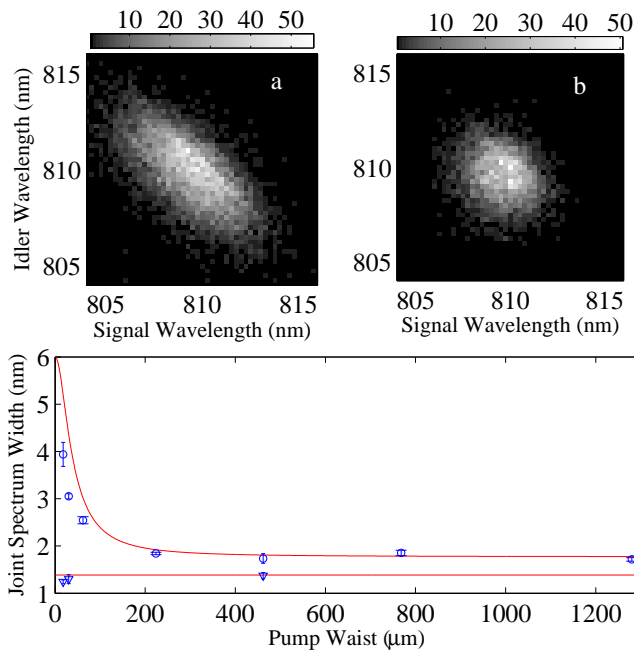


FIG. 4: Insets (a) and (b) corresponds to two different joint spectra measured for different pump waists. (a) $W_0 = 30 \mu\text{m}$, each point are coincidences measured in 50 s. (b) $W_0 = 462 \mu\text{m}$, each point are coincidences measured in 200 s. The curves in the lower part compares the theoretical prediction for the variation of $\Delta\Lambda_+$ and $\Delta\Lambda_-$ with W_0 , with experimental values. In all cases, the width of the Gaussian collection mode is $W_s = 133 \mu\text{m}$.

(a) of Fig. 4 corresponds to the case of frequency anti-correlated photons while part (b) of Fig. 4 corresponds to a two-photon state close to complete frequency uncorrelation. The values of the bandwidth measured for Fig. 4a are $\Delta\Lambda_+ = 1.29 \text{ nm}$ and $\Delta\Lambda_- = 3.05 \text{ nm}$, and for Fig. 4b, $\Delta\Lambda_+ = 1.37 \text{ nm}$ and $\Delta\Lambda_- = 1.73 \text{ nm}$.

In the lower part of Fig. 4, we compare the measured bandwidth for different pump beam waist, W_0 , with the theoretical prediction for our experimental parameters. From Eq. (4), one obtains that for large values of W_0 , $\Delta\Lambda_- \rightarrow \lambda_s^0/\omega_s^0\sqrt{2}/(N_s \tan \phi W_s)$. Under our experimental conditions, this asymptotic value is $\Delta\Lambda_-^\infty = 1.77 \text{ nm}$. On the other hand, the $\Delta\Lambda_+$ corresponding to the bandwidth of our pump laser is 1.38 nm . Therefore, the curves for $\Delta\Lambda_+$ and $\Delta\Lambda_-$ do not intersect, showing that our pump is not broad enough for achieving complete frequency correlated photon pairs with our W_s .

In conclusion, we have demonstrated experimentally the mapping of spatial characteristics imprinted on the pump beam into the joint spectrum of SPDC photons. Therefore, the generation of frequency shaped waveforms by spatially shaping the profile of the pump beam. Moreover, by making use of spatial light modulators, this technique could be used for the implementation of engineered multidimensional waveform alphabets with any type of frequency correlations.

We have extended this capability and we have shown the feasibility of tunable control of the frequency correlations of frequency-entangled two-photon states. The tuning parameter that mediates the control of the joint spectrum and consequently, the type of frequency correlations is the spatial beam waist of the pump. By changing this tuning parameter we observed photons with a highly reduced degree of frequency correlation. The role of the spatial collecting mode and the bandwidth of the pump beam in the generation of highly correlated photon pairs was also explained.

The technique to control the waveform of entangled photon pairs reported here can be of great interest for enhancing waveform control of paired photons generated through two-photon Raman transitions in electromagnetically induced transparency schemes[23], where highly noncollinear configurations are frequently used [24] and a rudimentary waveform control is demonstrated.

Acknowledgments

This work has been supported by EC under the integrated project Qubit Applications (QAP, IST directorate, Contract No. 015848), by the Government of Spain (Consolider Ingenio 2010 QIOT CSD2006-00019 and FIS2004-03556), and by the Generalitat de Catalunya.

* Electronic address: alejandra.valencia@icfo.es

† On the leave from Dip. di Fisica, Dipartimento di Fisica, Università di Camerino, I-62032 Camerino, Italy

‡ Also with ICREA-Institucio Catalana de Recerca i Estudis Avancats, 08010 Barcelona, Spain

§ Also with Department of Signal Theory and Communications, Universitat Politecnica de Catalunya, Barcelona, Spain

- [1] T. Aichele, A.I. Lvovsky, and S. Schiller, *Eur. Phys. J. D*, **18**, 237 (2002).
- [2] A. B. U'Ren et al., *laser. Phys.*, **15**, 146 (2005).
- [3] P. P. Rohde, T. C. Ralph, and M. A. Nielsen, *Phys. Rev. A* **72**, 052332 (2005).
- [4] W. P. Grice, A. B. U'Ren, and I. A. Walmsley, *Phys. Rev. A* **64**, 063815 (2001).
- [5] H. S. Poh et al., *Phys. Rev. A* **75**, 043816 (2007).
- [6] A. Valencia, G. Scarcelli, and Y. Shih, *App. Phys. Lett.* **85**, 2655 (2004).
- [7] V. Giovannetti, S. Lloyd, and L. Maccone, *Nature* **412**, 417 (2001).
- [8] C. K. Law, I. A. Walmsley, and J. H. Eberly, *Phys. Rev. Lett.* **84**, 5304 (2000).
- [9] O. Kuzucu, M. Fiorentino, M. A. Albota, F. N. C. Wong, and F. X. Kaertner, *Phys. Rev. Lett.* **94**, 083601 (2005).
- [10] J. P. Torres, F. Maci, S. Carrasco, and L. Torner, *Opt. Lett.* **30**, 314 (2005).

- [11] A. B. U'Ren, Reinhard K. Erdmann, Manuel de la Cruz-Gutierrez, and I.A. Walmsley, *Phys. Rev. Lett.* **97**, 223602 (2006).
- [12] Z. D. Walton, et al., *Phys. Rev. A* **67**, 053810 (2003).
- [13] A. B. URen, K. Banaszek, and I.A. Walmsley, *Quantum Inf. Comput.* **3**, 480 (2003).
- [14] S. Carrasco et al., *Phys. Rev. A* **73**, 063802 (2006).
- [15] L. Lanco et al., *Phys. Rev. Lett.* **97**, 173901 (2006)
- [16] M. C. Booth et al., *Phys. Rev. A* **66**, 023815 (2002).
- [17] A. De Rossi and V. Berger, *Phys. Rev. Lett.* **88**, 043901 (2002).
- [18] S. Carrasco et al., *Phys. Rev. A* **70**, 043817 (2004).
- [19] Y. H. Kim and W. P. Grice, *Opt. Lett.* **8**, 908 (2005).
- [20] F. A. Bovino et al., *Opt. Comm.*, **227**, 343 (2003).
- [21] C. Kurtsiefer, M. Oberparleiter, and H. Weinfurter, *Phys. Rev. A* **64**, 023802 (2001);
- [22] J. P. Torres, C. I. Osorio, and L. Torner, *Opt. Lett.* **29**, 1939 (2004).
- [23] V. Balic et al., *Phys. Rev. Lett.* **94**, 183601 (2005).
- [24] P. Kolchin et al., *Phys. Rev. Lett.* **97**, 113602 (2006).